



AFOSR - TR - 72 - 1104

A MULTIVARIATE DATA DISPLAY AND ANALYSIS PROCEDURE

Kenneth J. Breeding

AD 742283

The Ohio State University  
**ElectroScience Laboratory**

Department of Electrical Engineering  
Columbus, Ohio 43210

Technical Report 2768-7  
April 1972

Contract AFOSR 69-1710A

DDC  
RECEIVED  
MAY 29 1972  
RECEIVED  
C

Department of the Air Force  
Air Force Office of Scientific Research  
Arlington, Virginia 22209

Approved by  
NATIONAL TECHNICAL  
INFORMATION SERVICE

Approved for public release;  
distribution unlimited.

30  
A

NOTICES

When Government drawings, specifications, or other data are used for any purpose other than in connection with a definitely related Government procurement operation, the United States Government thereby incurs no responsibility nor any obligation whatsoever, and the fact that the Government may have formulated, furnished, or in any way supplied the said drawings, specifications, or other data, is not to be regarded by implication or otherwise as in any manner licensing the holder or any other person or corporation, or conveying any rights or permission to manufacture, use, or sell any patented invention that may in any way be related thereto.

COLLECTION For

OPBTI	WHITE SECTION	<input checked="" type="checkbox"/>
DDC	DIFF SECTION	<input type="checkbox"/>
UNANNOUNCED		<input type="checkbox"/>
JUSTIFICATION		
BY		
DISTRIBUTION/AVAILABILITY CODES		
DIST.	AVAIL.	SPECIAL
A		

## DOCUMENT CONTROL DATA - R &amp; D

(Security classification of title, body of abstract and indexing annotation must be entered when the overall report is classified)

1. ORIGINATING ACTIVITY (Corporate author) The Ohio State University Department of Electrical Engineering Columbus, Ohio 43212		2a. REPORT SECURITY CLASSIFICATION UNCLASSIFIED	
		2b. GROUP	
3. REPORT TITLE A MULTIVARIATE DATA DISPLAY AND ANALYSIS PROCEDURE			
4. DESCRIPTIVE NOTES (Type of report and inclusive dates) Scientific Interim			
5. AUTHOR(S) (First name, middle initial, last name) Kenneth J. Breeding			
6. REPORT DATE April 1972	7a. TOTAL NO. OF PAGES 26	7b. NO. OF REFS 9	
8a. CONTRACT OR GRANT NO. AFOSR 69-1710A		8b. ORIGINATOR'S REPORT NUMBER(S)	
b. PROJECT NO. 9769			
c. 61102F	8c. OTHER REPORT NO(S) (Any other numbers that may be assigned this report)		
d. 681304			
9. DISTRIBUTION STATEMENT Approved for public release; distribution unlimited.			
11. SUPPLEMENTARY NOTES TECH, OTHER		12. SPONSORING MILITARY ACTIVITY Air Force Office of Scientific Research(NM) 1400 Wilson Boulevard Arlington, Virginia 22209	
13. ABSTRACT This paper seeks to extend the conventional linear, and non-linear, feature space mappings used in pattern recognition. Of particular interest when data are highly interdependent, the minimal spanning trees of Zahn are shown to contain a great deal of information about the distribution of this type of data. Further, trees are shown to be indicative of the quantization level necessary for application of nearest neighbor recognition schemes. A linear projection is developed to display the data and confirm distributions applicable to the minimal spanning trees.			

A MULTIVARIATE DATA DISPLAY AND ANALYSIS PROCEDURE

Kenneth J. Breeding

Technical Report 2768-7  
April 1972

Contract AFOSR 69-1710A

Department of the Air Force  
Air Force Office of Scientific Research  
Arlington, Virginia 22209

Approved for public release;  
distribution unlimited.

## CONTENTS

	Page
I. INTRODUCTION	1
II. BASIC DEFINITIONS	2
III. DATA DISTRIBUTION INFERENCE FROM MST's	5
IV. A TWO DIMENSIONAL LINEAR PROJECTION	12
V. CONCLUDING REMARKS	20
REFERENCES	21
APPENDIX A	23

## I. INTRODUCTION

One of the difficulties in dealing with n-dimensional feature vectors in pattern recognition is the identification of the way in which the data is distributed in the space. If this distribution is known, then the recognition problem may generally be solved by use of discriminant functions which take advantage of this distribution.<sup>1</sup> An excellent example of the way in which this may be done is the OLPARS system.<sup>2</sup> There have been a number of algorithms presented in the literature which offer displays in two or three dimensions of the distribution of n dimensional data. A few of these techniques are presented by Sammon.<sup>3</sup> The majority of such techniques appear to be nonlinear. Sammon,<sup>4</sup> Ball,<sup>5</sup> and Shepard and Carroll<sup>6</sup> present several examples of nonlinear mappings.

The objective of the display mappings is to preserve some specified characteristic of the data distribution. One such characteristic which is very desirable in pattern recognition is linear separability. The objective for projection of two classes of data, then, is to maintain this interclass separability. An approach which projects the data set onto a plane oriented in such a way as to maximize this interclass separation has been suggested by Sammon.<sup>7</sup> This technique uses the Fisher Discriminant<sup>8</sup> to determine one of the axes of projection. The second axis is determined by maximizing the data spread on the projecting plane. This mapping is a linear one. Fukunaga and Olsen<sup>9</sup> present a similar approach which is nonlinear in nature.

A fundamentally different approach to this problem was presented by Zahn<sup>10</sup> in 1971. In his paper, Zahn suggests that graph theoretic methods may be used to detect and describe data clustering. Basically this approach computes a minimal spanning tree for the data clusters. A "stylized" two dimensional drawing of such a tree then gives some information about data distribution, primarily inter-point distances.

In all of the techniques described above, no cognizance has been made of the functional interdependence of data. Many problems have data which are highly interdependent. Examples of this

are pattern recognition problems which use multivariate feature vectors to describe two or three dimensional objects at a succession of aspects or view angles.<sup>11, 12</sup>

In cases such as these highly structured data would be expected. In particular, the  $n$  dimensional feature vectors describing a two dimensional object would be expected to form a line trajectory in  $n$  space as the two dimensional object is rotated. Similarly the trajectory of the description for 3 dimensional objects should form a surface as the object is rotated.

Although each of the projection techniques described above are capable of handling such data, no effort has been made to exploit these characteristics.

In what follows, it will first be shown that the minimal spanning trees of Zahn contain a great deal of information about the distribution of data of this type. Further these trees will be shown to be indicative of the quantization level necessary for application of nearest neighbor recognition schemes. Finally, a linear projection scheme similar to that of Reference 7 will be used to display the data and confirm distributions suggested by the minimal spanning trees.

## II. BASIC DEFINITIONS

Before proceeding to the algorithms, some fundamental definitions are required. For a more complete discussion of graph theory see Reference 13. A linear graph is composed of a set,  $V$ , of vertices or nodes and a set,  $E$ , of vertex pairs, called edges, which describe the intersection of vertices. Whenever a number, called an edge weight, is associated with each edge the resulting linear graph is called an edge weighted linear graph. A path in a graph is a sequence of edges joining two nodes. Typically a path is described by the sequence of vertices which define the edges of the path. Figure 1 shows an edge weighted linear graph with a path (ABGFD).

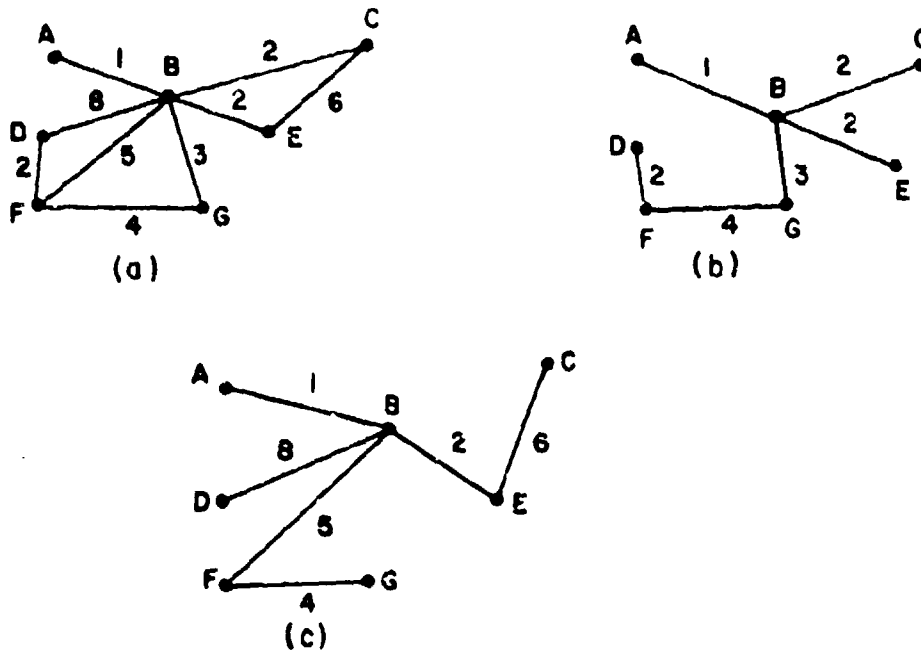


Fig. 1. Edge weighted linear graphs and some trees.

A circuit is a closed path such as (DBFD) in Fig. 1. If a graph has a path between every pair of nodes, then it is said to be connected. A strongly connected graph is a connected graph in which any pair of nodes is connected by an edge. A tree is a connected graph having no circuits and a spanning tree of a graph  $G$  is a tree in  $G$  which contains all nodes of the graph  $G$ . An example of such a tree for the graph of Fig. 1(a) is shown in Fig. 1(b). Another spanning tree is shown in Fig. 1(c). In general, the total number of trees for a given graph is quite large. For edge weighted linear graphs a useful subclass of all the spanning trees is the class of trees called a minimal spanning trees defined as follows. Let the weight of a tree be defined as the



sum of the weights of its constituent edges. Then a minimal spanning tree is a spanning tree having the lowest weight.

Figure 1(b) shows a minimal spanning tree or MST, for the graph of Fig. 1(a). It should be noted that, in general, a given graph may not have a unique minimal spanning tree.

A number of algorithms exist for computing the minimal spanning tree of a graph. Two of these procedures, given in 1956 and 1957 by Krushal<sup>14</sup> and Prim<sup>15</sup> respectively, are remarkably straight forward. Krushal's algorithm begins by listing the edges of the graph G in order of ascending weight. For example this list becomes for Fig. 1(a).

<u>EDGE</u>	<u>WEIGHT</u>	<u>SELECTION</u>
AB	1	X
BC	2	X
BE	2	X
DF	2	X
BG	3	X
FG	4	X
BF	5	
CE	6	
BD	8	

Starting with the topmost edge (least weight) select edges in order in such a way that no circuits are formed with edges already selected. The process stops when  $n-1$  edges have been chosen, where  $n$  is the number of nodes in the graph. Following this selection process, the spanning tree of Fig. 1(b) is shown to be an MST for the graph of Fig. 1(a).

The algorithm of Prim is equally as simple. Start with any node and add the edge connected to this node having the least weight. This edge taken with its end points forms a fragment tree,  $T_1$ .  $T_k$  is obtained from  $T_{k-1}$  by adding the shortest edge connecting a node in G but not in  $T_{k-1}$ . The procedure terminates on tree  $T_{n-1}$ . Consider as an example Fig. 1(a). Applying this process to this graph the following table summarizes the steps.

<u>NODES</u>	<u>EDGE ADDED</u>	<u>WEIGHT</u>
A	AB	1
A, B	BC	2
A, B, C	BE	2
A, B, C, E	BG	3
A, B, C, E, G	GF	4
A, B, C, E, G, F	DF	2
A, B, C, E, G, F, D	Stop	

Zahn shows in his paper<sup>10</sup> a number of ways in which the minimal spanning tree of a graph may be used to describe and identify data clustering. For data which is functionally interdependent, data clustering, of the type suggested by Zahn, will occur only when data samples are spaced far apart. In the next section this problem will be defined more precisely and it will be shown that such an observation may be used to identify data trajectory and help set a quantization level on the data used to represent an object class for pattern recognition purposes.

### III. DATA DISTRIBUTION INFERENCE FROM MST's

Let  $S = \sigma_1, \sigma_2, \dots, \sigma_k$  be a set of  $k$  object classes which are to be recognized. Associated with each object class is a set of  $n$ -tuples,  $A_{\sigma_i}$ , called features, which are taken to represent object class  $\sigma_i$ , at some given set of aspects or view angles. For the discussion to follow, the aspect angles will be defined as the normal spherical coordinate angles  $\phi$  and  $\theta$  shown in Fig. 2. Thus, the set of points in  $A_{\sigma_i}$

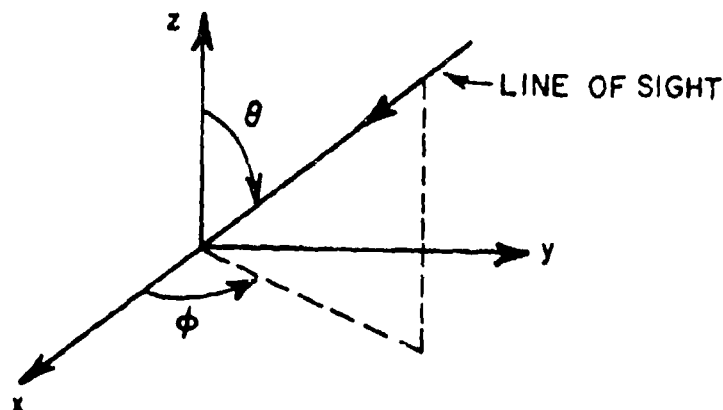


Fig. 2. Aspect angle convention.

represent points on an n-dimensional surface which is formed by the locus of the feature vectors as the aspect angles change. (This assumes noiseless feature measurements.) The set of points  $A_{\sigma_i}$  may now be taken as the vertices of a strongly connected graph, i.e., all points in  $A_{\sigma_i}$  are connected to all other points in  $A_{\sigma_i}$  by edges. Further, the Euclidean distance between any two n-tuples or features in  $A_{\sigma_i}$ ,  $\bar{X}$  and  $\bar{Y}$ , may be taken as the weight for the corresponding, connecting edge. Thus  $A_{\sigma_i}$  represents an edge weighted, strongly connected linear graph.

Next let  $A_{\sigma_i}^*$  be the ordered set formed from  $A_{\sigma_i}$  by an ordering induced on the vectors  $A_{\sigma_i}$  by aspect angles as follows

$$(1) A_{\sigma_i}^* = \langle \vec{X}_{0,0}^{(i)}, \vec{X}_{0,1}^{(i)}, \dots, \vec{X}_{0,\alpha_1}^{(i)}, \vec{X}_{1,0}^{(i)}, \dots, \vec{X}_{1,\alpha_1}^{(i)}, \dots, \vec{X}_{j,l}^{(i)}, \dots \rangle$$

where

$$(2) \vec{X}_{j,\ell}^{(i)} = f_i(\phi_j, \theta_\ell) \quad \text{and where}$$

and

$$(3) \phi_j \geq \phi_{j-1}$$

$$(4) \theta_\ell \geq \theta_{\ell-1}.$$

Define an ordered  $\phi_j$  or  $\theta_\ell$  subset of  $A_{\sigma_i}^*$ , denoted by  $S_{\phi_j}(\sigma_i)$  or  $S_{\theta_\ell}(\sigma_i)$ .

as

$$(5) S_{\phi_j}(\sigma_i) = \langle \vec{X}_{j,0}^{(i)}, \vec{X}_{j,1}^{(i)}, \dots, \vec{X}_{j,\alpha_j}^{(i)} \rangle$$

$$(6) S_{0, \ell}(\sigma_i) = \langle \vec{X}_{0, \ell}^{(i)}, \vec{X}_{1, \ell}^{(i)}, \dots, \vec{X}_{\beta_s, \ell}^{(i)} \rangle$$

where

$$(7) \vec{X}_{j, q}^{(i)} \in A_{\sigma_i}, \quad q = 0, 1, 2, \dots, \alpha_r$$

$$(8) \vec{X}_{\rho, \ell}^{(i)} \in A_{\sigma_i}, \quad \rho = 0, 1, 2, \dots, \beta_s.$$

Thus

$$(9) A_{\sigma_i} = \langle S_{\phi_0}(\sigma_i), S_{\phi_1}(\sigma_i), \dots, S_{\phi_\zeta}(\sigma_i) \rangle$$

where  $\zeta$  is the number of different  $\phi$  aspect angles in the set  $A_{\sigma_i}$ . Note that if an object,  $\sigma_i$ , has cylindrical symmetry with the axis of symmetry co-linear with z-axis then

$$(10) S_{\phi_\mu}(\sigma_i) = S_{\phi_\nu}(\sigma_i) \text{ for all } \mu \text{ and } \nu.$$

and

$$(11) A_{\sigma_i}^* = \langle S_\phi(\sigma_i) \rangle.$$

In general the  $S_\phi(\sigma_i)$  may be considered as sets of points in n-space located on the line formed by the locus of points having  $\phi$  fixed and  $\theta$  varying over all possible values. Consider now the MST formed from  $S_\phi(\sigma_i)$  as described earlier. For simplicity let

$$(12) \quad S_\phi(\sigma_i) = \langle \vec{X}_1^{(i)}, \vec{X}_2^{(i)}, \dots, \vec{X}_l^{(i)} \rangle.$$

Now if the features,  $\vec{X}_j^{(i)}$ , are selected with  $\theta$  increments sufficiently close to each other, then the minimal spanning tree will be defined by connecting  $\vec{X}_1^{(i)}$  to  $\vec{X}_2^{(i)}$  and  $\vec{X}_2^{(i)}$  to  $\vec{X}_3^{(i)}$  and so on to  $\vec{X}_{l-1}^{(i)}$  to  $\vec{X}_l^{(i)}$ . On the other hand, if the  $\theta$  increments are fairly large, it is easily seen that this minimal spanning tree will, in general, not occur. As an example consider Fig. 3(a). Suppose that ten points, numbered 1 through 10 are chosen to represent the curve shown and thus define  $S_\phi(\sigma)$ . The minimal spanning tree for this function is shown in Fig. 3(b). Note that because of the large increments in  $\theta$ , the points are not connected consecutively in the MST. If, on the other hand, the increments were chosen smaller as in Fig. 3(c) then the resulting MST will have the points sequentially spaced as shown in Fig. 3(d).

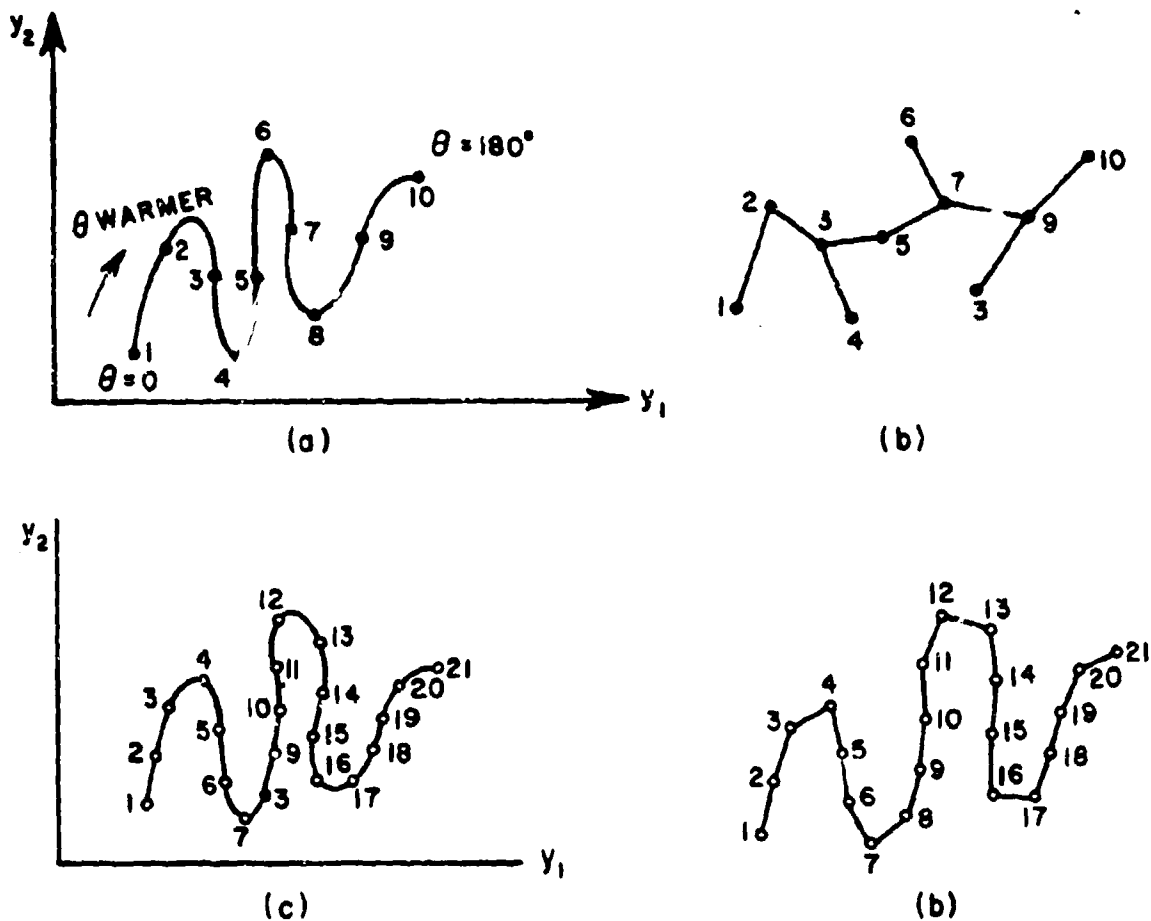


Fig. 3. Quantization effects on the MST of a data set.

As indicated by this example, the MST may be used to indicate the degree of quantization in aspect angle required to properly represent the object class. This is, of course, purely a qualitative measure of accuracy of representation and is intended to be nothing more. There is, however, more information in the MST than simply quantization levels. The MST carries a good deal of information about structure as well. As an example of this the multifrequency backscatter return amplitudes for the step cylinder described in Appendix A were obtained. Seven data points in 8-space were taken corresponding to  $\theta$  of  $0^\circ$ ,  $30^\circ$ ,  $60^\circ$ ,  $\dots$ ,  $180^\circ$ . These points are labeled 1, 2,  $\dots$ , 7 respectively. A stylized version of the minimal spanning tree for this data is shown in Fig. 4(a). Note that the data points are not consecutively arranged in the MST, thus indicating a coarse quantization level. However, this coarseness makes possible the rough identification of data trajectory, since the data points should lie consecutively on the locus of points formed by varying  $\theta$  through all possible values. Thus it may be

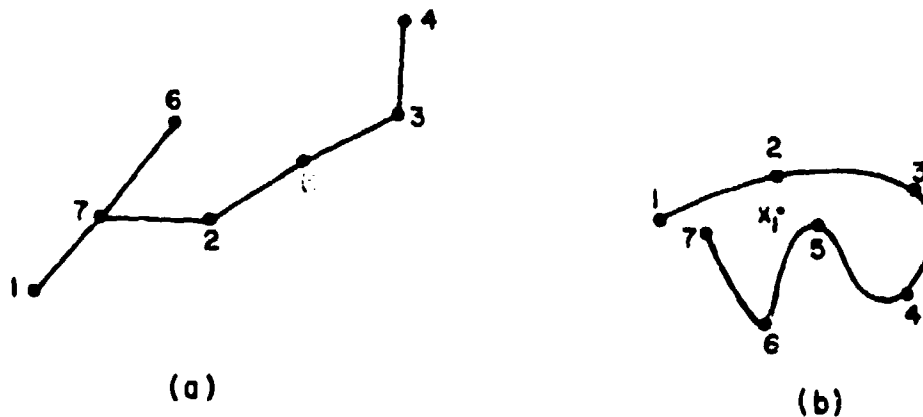


Fig. 4. MST for step cylinder and inferred trajectory.

inferred from the MST that because points 1 and 7 are adjacent the trajectory must be folded back. This is, of course, what one expects since the step cylinder has the same cross section from look angles  $\theta = 0^\circ$  or  $\theta = 180^\circ$ . In a similar way note that points 3 and 5, corresponding to  $\theta = 60^\circ$  and  $\theta = 120^\circ$  respectively are adjacent as would be expected from the symmetry of the target.

It may then be seen that the MST does indicate in some sense the data trajectory. More to the point, however, the minimal spanning tree allows one to identify those aspect angles at which the target object shows a similar views or cross sections. With proper quantization, this observation may be carried to multiple objects. For example, the data for the cylinder and prolate spheroid described in Appendix A were combined to form one data set from which the minimal spanning tree was computed. The data points were labeled 1 to 10 for the cylinder data and 11 to 20 for the prolate spheroid. The corresponding aspect angles were  $\theta = 0^\circ, 10^\circ, 20^\circ, \dots, 90^\circ$  in both cases. Figure 5 shows the corresponding MST and the inferred distribution. These figures suggest that at an aspect angle of something like  $40^\circ$  to  $50^\circ$

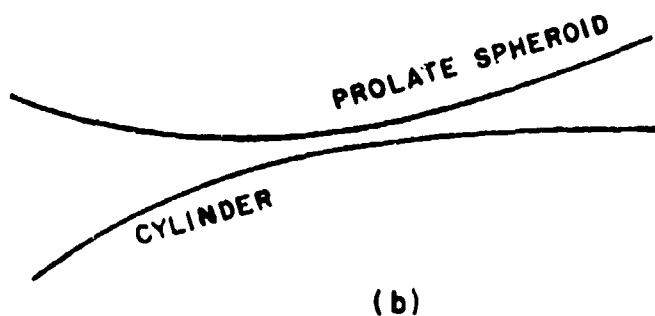
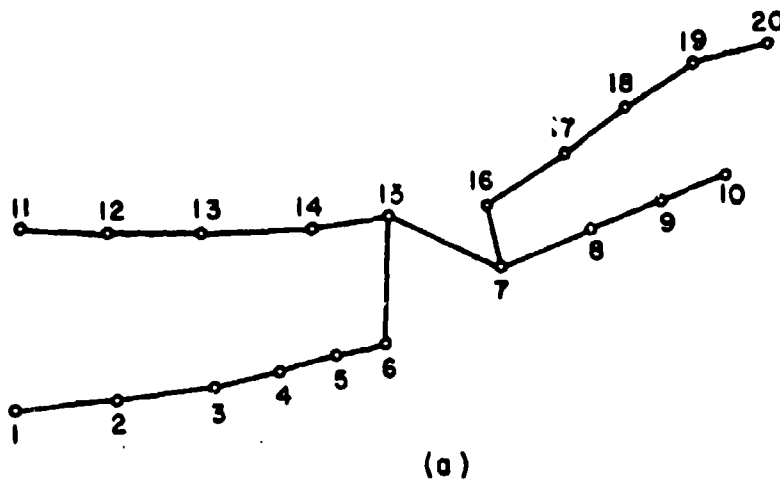


Fig. 5. MST and inferred trajectory for combined prolate spheroid and cylinder data.

I

the two objects appear more alike than at other aspects. It does not imply that the targets look the same; only that they look more alike at this aspect than others. It will be shown below that the inferred trajectories are probably correct.

Before discussing the linear transformation of the data, a few comments on application of the minimal spanning tree are in order. One of the very useful pattern recognition techniques is application of a nearest neighbor rule for identification. One such rule identifies an unknown vector,  $\bar{X}$ , as belonging to class  $\sigma_i$  if  $\bar{X}$  is nearer some vector in  $A_{\sigma_i}$ ,  $\bar{a}_i$ , than any vector in any other  $A_{\sigma_j}$ . Two pieces of information are thus obtained. The first is object identification. The second is object orientation with respect to the viewer. If the aspect angle quantization is small enough then the target orientation is easily and accurately obtained by assigning it as the orientation associated with vector  $\bar{a}_i$ . Dudani<sup>12</sup> effectively does this in his recognition schemes using moment invariants. If on the other hand, this quantization is fairly coarse then the accuracy of the orientation estimate is questionable. For example assume the point to be identified is the one marked X in Fig. 4(b). This point is closer to point 2 than 5 and this would be assigned an orientation corresponding to point 2. In fact, X is closer to a point on the line connecting point 5 and 6 than it is to either point 2 or 5. If the quantization had been smaller the error in orientation could thus have been avoided. To set this quantization one needs only to repeatedly decrease the  $\theta$  increment until the minimal spanning tree has contiguous points in contiguous locations in the tree. It should be noted that this quantization may be set locally rather than the globally, i.e., the minimum  $\theta$  increments required may be different for different regions in the data trajectory.

Such a quantization level is too fine, however, for investigation of data trajectory. The reason for this is that the minimal spanning tree is simply a listing of interconnected nodes and is not an actual visual display. Thus a fine quantization simply says that point 1 is connected to point 2 and 2 is connected to 3 and so on which was known to begin with. By making a fairly coarse quantization, the points in the MST may no longer be located consecutively and thus give information concerning the data trajectory by inference from these noncontiguous points.



#### IV. A TWO DIMENSIONAL LINEAR PROJECTION

The use of the minimal spanning tree to identify data trajectory is qualitative by nature and allows for a good deal of subjective analysis. What is needed then is some approach which may be used to supply some form of quantitative information about data distribution. This approach should not introduce appreciable distortion in the display and therefore probably should be linear. For the case of two data classes a very nice approach was proposed by Sammon<sup>7</sup> using the Fisher discriminant<sup>8</sup>. This approach is not readily adaptable to a one class problem. In order to handle such a problem a new approach is needed.

Basically the main requirement on the projection plane is that the projected data be spread out on the plane as much as possible, i.e., the standard deviation should be as large as possible. One procedure by which this ideal situation may partially be accomplished is described below. The choice of the algorithm has been devised to meet two requirements. First, it should give a fairly large projected data spread. This spread need not be maximal in any sense. Secondly, and most importantly, the projection plane axis should be easily determined. Thus the following algorithm is heuristically derived.

One way in which a projection hyperplane may be chosen so as to produce a large spread in the data is, at least intuitively, to project the  $n$  dimensional data points into some two dimensional subspace of an  $n-1$  dimensional hyperplane oriented along the direction of data spread. The hyperplane through the data spread may be thought of in the same way as one thinks of the plane of the Milky Way. More specifically, this plane is defined by the vector  $\omega^{(1)}$  such that  $z_1$  is minimized where

$$(13) \quad z_1 = \sum_{i=1}^S [ (\vec{x}^{(i)} - \bar{\rho}) \cdot \vec{\omega}^{(1)} ]^2$$

and where\*

$$(14) \quad s = |A_\sigma|$$

$$(15) \quad \vec{p} = \frac{1}{s} \sum \vec{\alpha}^{(i)}$$

for all  $\vec{\alpha}^{(i)} \in A_\sigma$ .

The minimization problem (13) will be trivially solved by the zero vector so some constraint needs to be added to insure a nonzero solution. In the vast majority of cases, the spread hyperplane will not contain the first moment vector  $\vec{p}$ , i.e., most of the time  $\vec{p} \cdot \vec{\omega}^{(1)} \neq 0$ . Thus a constraint of  $\vec{p} \cdot \vec{\omega}^{(1)} = 1$  may be added to (13) using a Lagrange multiplier to produce the following optimization problem.

$$(16) \quad \text{Min } z_1 = \sum_{i=1}^s [(\vec{\alpha}^{(i)} - \vec{p}) \cdot \vec{\omega}^{(1)}]^2 + \lambda_1 (1 - \vec{\omega}^{(1)} \cdot \vec{p})$$

By setting the partial derivatives of  $z_1$  with respect to  $\lambda_1$ , and  $\omega_i^{(1)}$ ,  $i = 1, 2, \dots, n$  to zero and solving the resulting system of equations,  $\vec{\omega}^{(1)}$  may be obtained.

The next problem is to determine an appropriate two dimensional subspace of the hyperplane defined by  $\vec{\omega}^{(1)}$ . One way of doing this (and the way chosen here arbitrarily) is to define an  $n-1$  orthonormal basis  $\vec{\omega}^{(2)}, \dots, \vec{\omega}^{(n)}$  in  $\vec{\omega}^{(1)}$  such that the vectors  $\vec{\omega}^{(1)}, \vec{\omega}^{(2)}, \dots, \vec{\omega}^{(n)}$  are mutually perpendicular. This may be done iteratively as follows.

---

\* The order of a set X is denoted by  $|X|$ .

$$(17) \text{ Min } z_{\kappa} = \sum_{i=1}^n [(\bar{\alpha}^{(i)} - \bar{\rho}) \cdot \bar{\omega}^{(\kappa)}]^2 + \lambda_1 (1 - \bar{\omega}^{(\kappa)} \cdot \bar{\rho})$$

$$+ \sum_{\ell=1}^{\kappa-1} \lambda_{\ell} \bar{\omega}^{(\ell)} \cdot \bar{\omega}^{(\kappa)}, \quad \kappa = 2, 3, \dots, n$$

The system of equations arising by setting to zero the appropriate partial derivative of  $z_{\kappa}$  become

(18)

$$\begin{bmatrix} 0 \\ 0 \\ \cdot \\ \cdot \\ \cdot \\ 0 \\ -1 \\ 0 \\ 0 \\ \cdot \\ \cdot \\ \cdot \\ 0 \end{bmatrix} = \begin{bmatrix} c_{11} \cdots c_{1n} - \rho_1 \omega_1^{(1)} \cdots \omega_1^{(\kappa-1)} \\ \cdot \quad \cdot \quad -\rho_2 \omega_2^{(1)} \cdots \omega_2^{(\kappa-1)} \\ \cdot \quad \cdot \quad \cdot \quad \cdot \\ \cdot \quad \cdot \quad \cdot \quad \cdot \\ \cdot \quad \cdot \quad \cdot \quad \cdot \\ c_{n1} \cdots c_{nn} - \rho_n \omega_n^{(1)} \cdots \omega_n^{(\kappa-1)} \\ -\rho_1 \quad \cdots \quad -\rho_n \\ \omega_1^{(1)} \quad \omega_n^{(1)} \\ \omega_1^{(2)} \quad \omega_n^{(2)} \quad \quad \quad 0 \\ \cdot \quad \cdot \\ \cdot \quad \cdot \\ \cdot \quad \cdot \\ \omega_1^{(\kappa-1)} \cdots \omega_n^{(\kappa-1)} \end{bmatrix} \begin{bmatrix} \omega_1^{(\kappa)} \\ \omega_2^{(\kappa)} \\ \cdot \\ \cdot \\ \cdot \\ \omega_n^{(\kappa)} \\ \lambda_1 \\ \lambda_2 \\ \cdot \\ \cdot \\ \lambda_{\kappa} \end{bmatrix}$$

A solution to (18) thus gives the  $\kappa$ th vector  $\vec{\omega}^{(\kappa)}$ .  
 The two dimensional projection plane is finally taken as defined  
 by  $\vec{\omega}^{(n)}$  and  $\vec{\omega}^{(n-1)}$ . The projection is then made as

$$(19) \quad X_i = \vec{\alpha}^{(i)} \cdot \vec{\omega}^{(n)}$$

$$(20) \quad Y_i = \vec{\alpha}^{(i)} \cdot \vec{\omega}^{(n-1)}$$

for  $i = 1, 2, \dots, S$ , i.e., for all  $\alpha^{(i)} \in A_{\sigma}$ .

Figures 6, 7, and 8 show the data for the step cylinders prolate spheroid and the cylinder respectively as projected onto planes derived as just described. Note that the data trajectory is clearly shown and further that the trajectory of the step cylinder data is, indeed, similar to the inferred trajectory as shown in Fig. 4(b).

If two classes exist then the above procedure may be used for display after suitable modification. In this case, normally, the important criteria is maintenance of linear separation in the projected image. Maximizing the data spread thus becomes secondary. To accomplish these goals  $\vec{\omega}^{(1)}$  may be taken as a separating hyperplane for the two classes or some "near" separating hyperplane if the classes are not linearly separable. Applying the procedure described above, the projection axes then are taken as  $\vec{\omega}^{(1)}$  and  $\vec{\omega}^{(n)}$  in equations (19) and (20) respectively. The hyperplane  $\vec{\omega}^{(1)}$  may be found in a number of ways such as the Fisher discriminant mentioned earlier, linear programming<sup>16</sup>, or an adoptive approach such as described in Reference 11. Using the latter, the above projection technique was applied to the combined prolate spheroid/cylinder data. The resulting projection is shown in Fig. 9. Note, first, that the separation of the two classes is clearly shown and, secondly, the similarity to the inferred trajectories of Fig. 5(b). As a further reference, compare Fig. 3 with the individual trajectories for the cylinder and prolate spheroid shown respectively in Fig. 7 and 8.

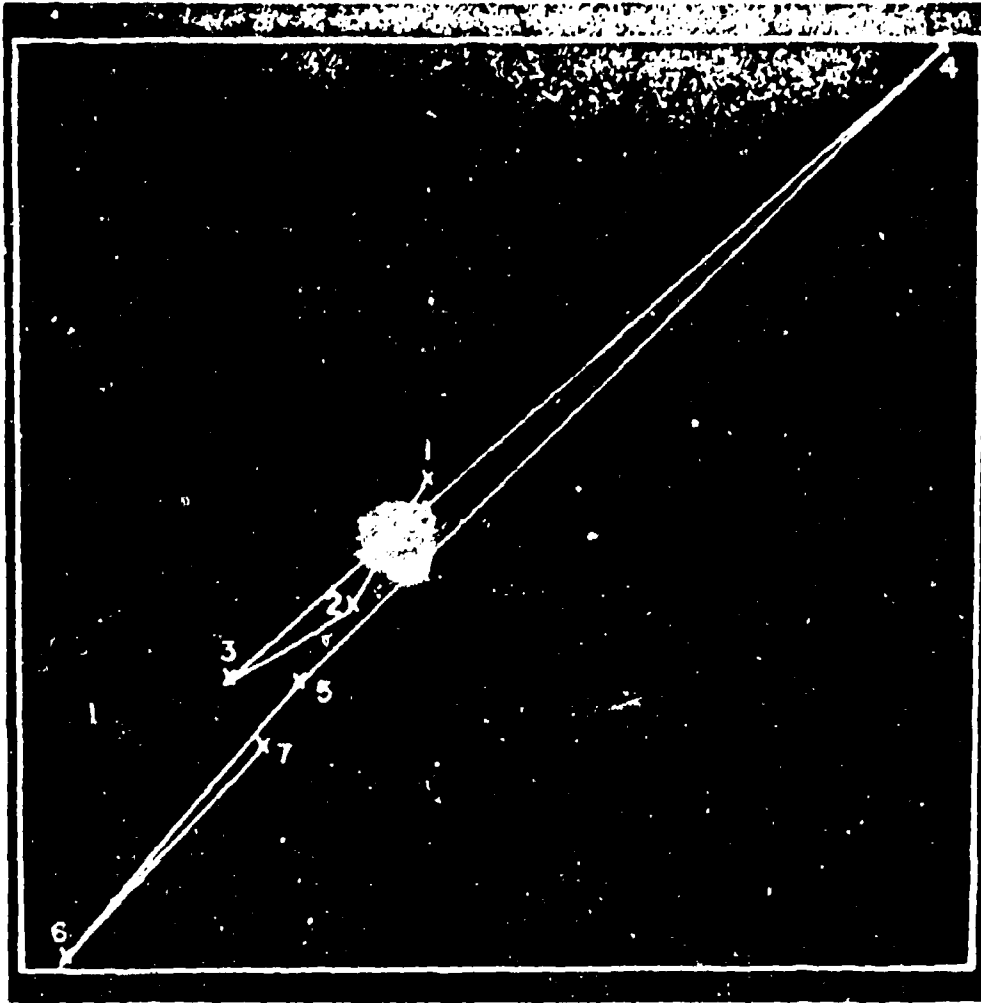


Fig. 6. Step cylinder data projection.

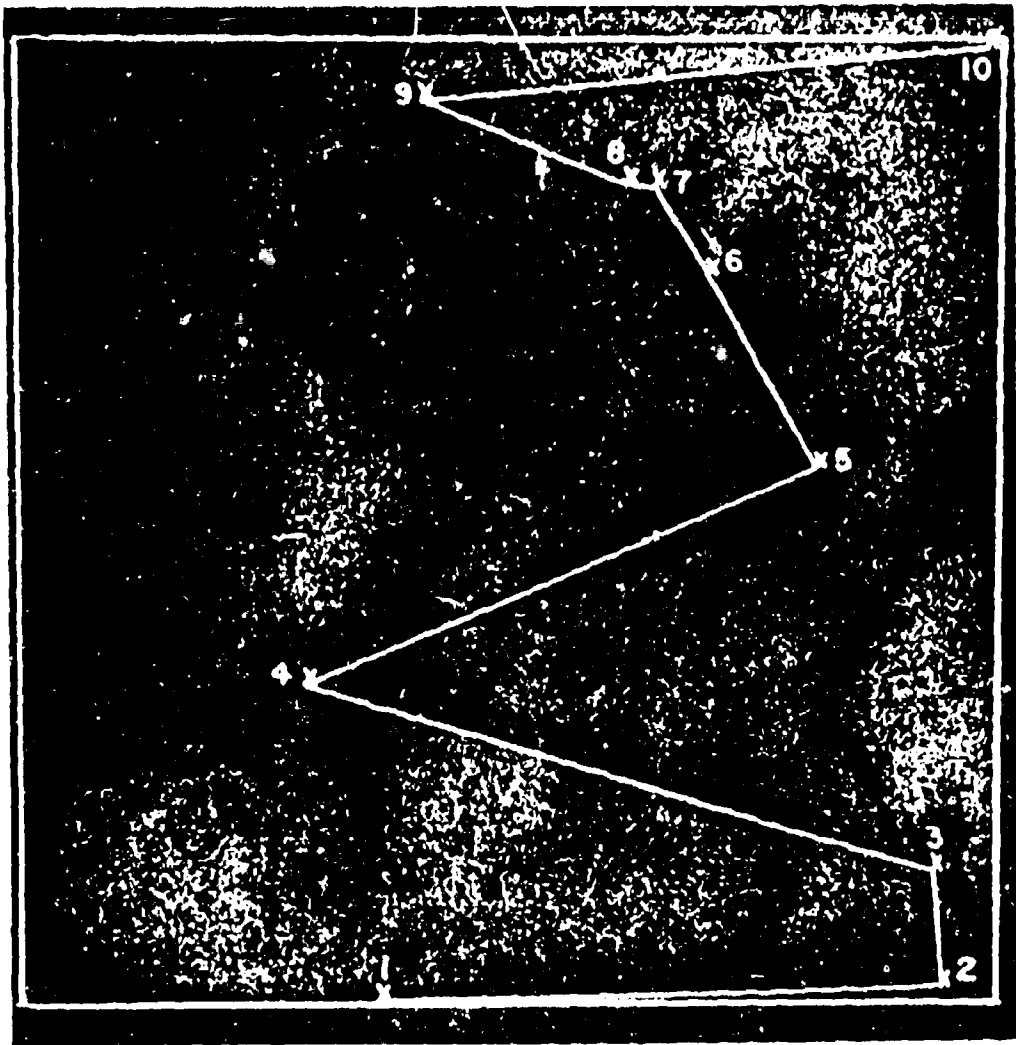


Fig. 7. Cylinder data projection.

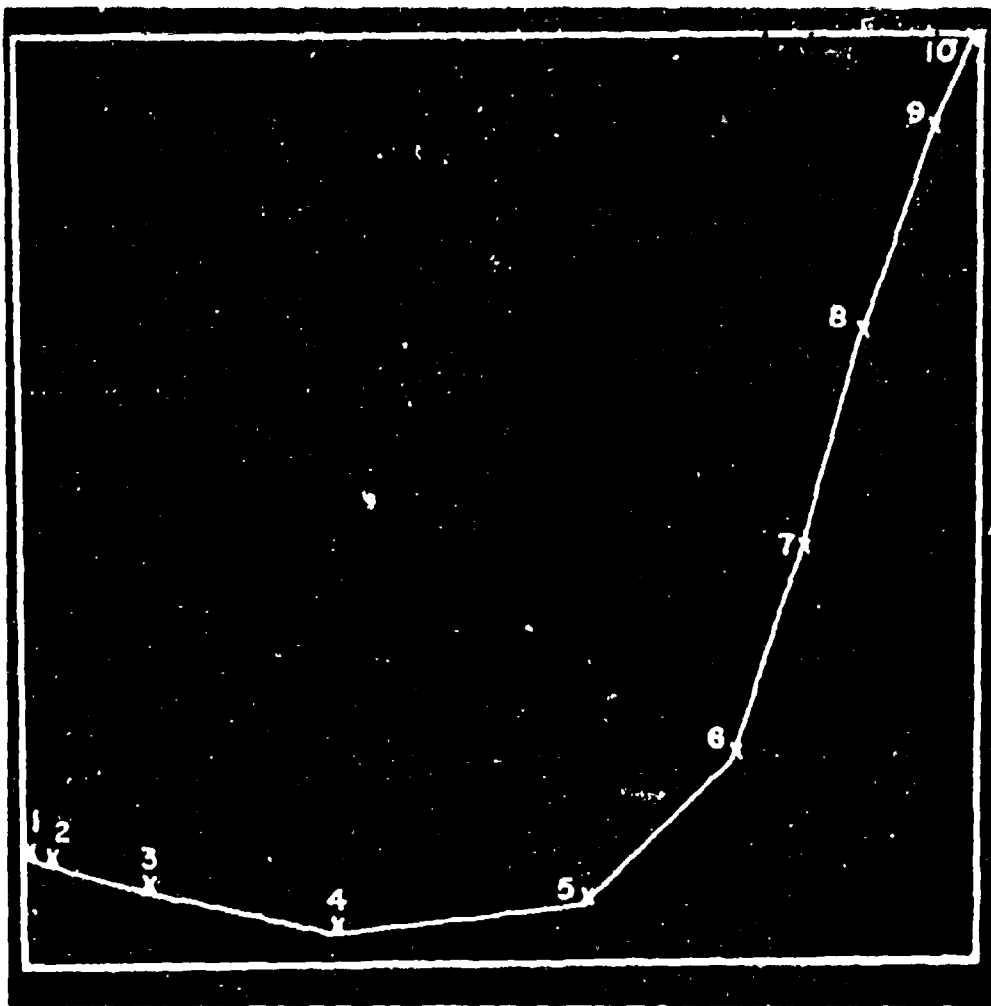


Fig. 8. Prolate spheroid data projection.

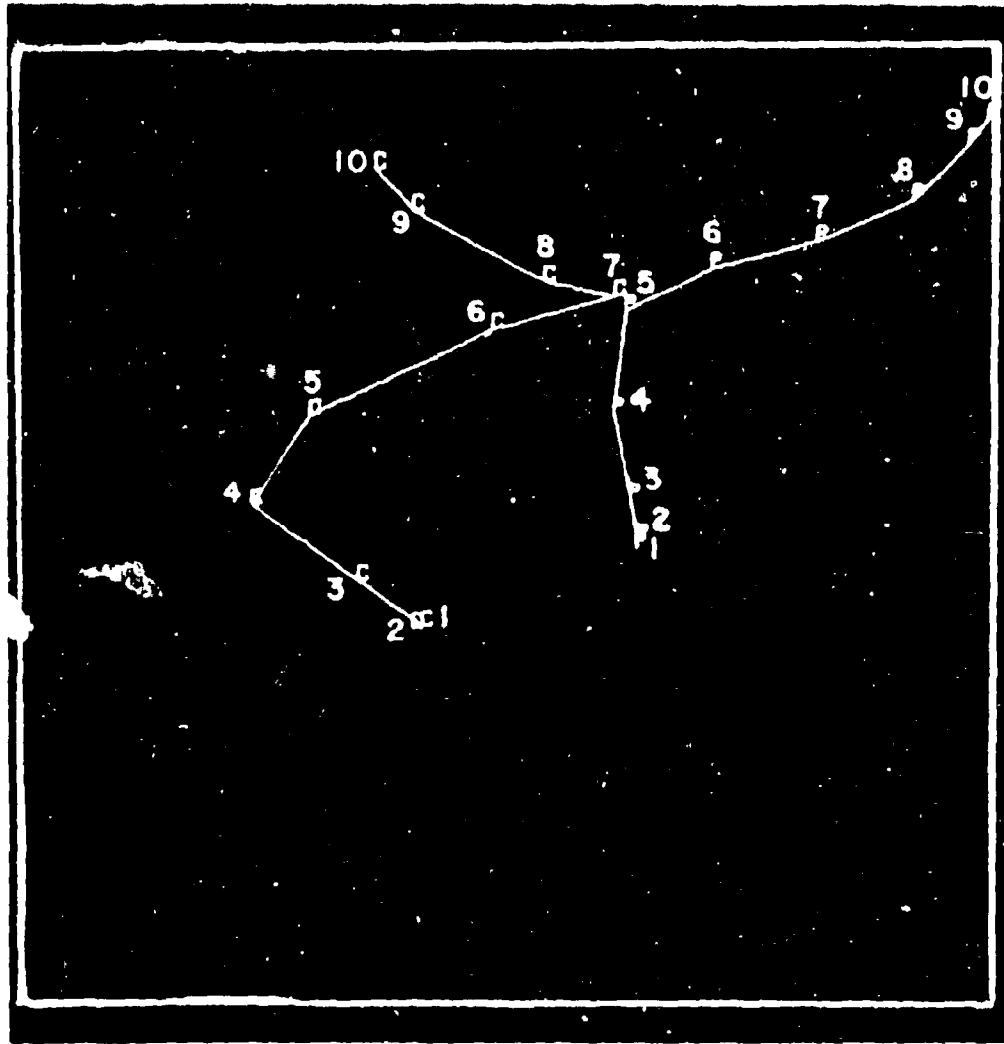


Fig. 9. Cylinder/prolate spheroid data projection.



## V. CONCLUDING REMARKS

This report has dealt with two methods of multivariate data analysis which have been effectively used to represent functionally related data structures. Taken together they offer the user a method of visualizing data structure and thereby providing some insight into the problem encountered in attempting to classify or recognize an unknown target object.

In particular there are two areas related to pattern recognition where a thorough knowledge of data trajectory becomes of great value. The first has to do with the actual identification of the target object from a knowledge of the target data trajectory. By comparing this unknown trajectory with a set of known ones an identification may be possible on the basis of similar trajectory shapes. This becomes especially important in cases where there is a significant overlap in data between two or more object classes. Much work is yet to be done in this area.

The second application area has to do with the identification of target aspect from a knowledge of target identification and target data trajectory. By matching up the measured trajectory with some portion of the known data trajectory to obtain a best fit the temporal orientation of the target may be inferred, i.e., one can identify the trajectory of the target object relative to the observer.

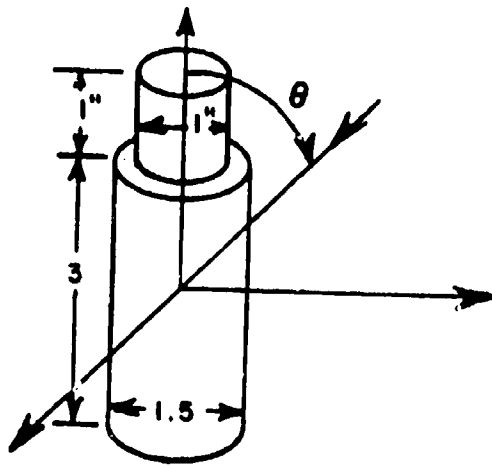
From these applications, it is clear that a knowledge of data trajectory allows one to obtain greater confidence in a given identification as well as help in choosing a particular recognition algorithm to be used with a particular data set. The data analysis algorithm described here is intended to help in such determinations.

## REFERENCES

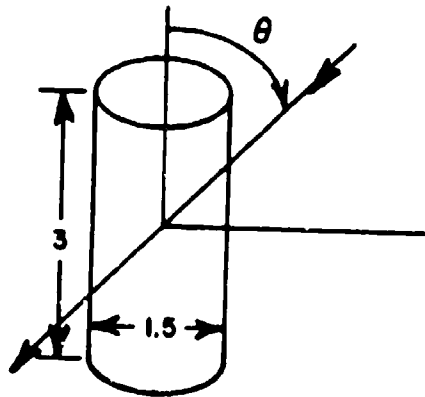
1. Nilson, N.J., Learning Machines: Foundation of Trainable Pattern Classifying Systems, McGraw-Hill, New York, 1965.
2. Sammon, J.W. Jr., "On Line Pattern Analysis and Recognition System (OLPARS)," Rome Air Development Center, Rome, New York, Tech. Rept. RADC-TR-68-263, August 1968.
3. Sammon, J.W. Jr., "Interactive Pattern Analysis and Classification," IEEE TC, Vol. C-19, pp. 594-616, July 1970.
4. Sammon, J.W. Jr., "A Nonlinear Mapping for Data Structure Analysis," IEEE TC, Vol. C-18, pp. 401-409, May 1969.
5. Ball, F.H., "Data Analysis in the Social Sciences: What about the Details?" AFIPS Conf. Proc. 1965, Fall Joint Computer Conference, pp. 533-559.
6. Shepard, R.N. and Carroll, J.D., "Parametric Representation of Nonlinear Data Structures," Proc. Int. Symp. Multivariate Analysis, Ed. by P.R. Krishmarah, Academic Press, New York, 1966.
7. Sammon, J.W. Jr., "An Optical Discriminant Plane," IEEE TC, Vol. C-19, pp. 826-829, September 1970.
8. Fisher, R.A., "The Use of Multiple Measurements in Taxonomic Problems," Ann. Engrn., Vol. 7, pp. 179-188, September 1936.
9. Fukunoga, K. and Olsen, D.R., "A Two-Dimensional Display for the Classification of Multivariate Data," IEEE TC, Vol. C-20, pp. 917-923, August 1971.

10. Zahn, C.L., "Graph-Theoretical Method for Detecting and Describing Gestalt Clusters," IEEE TC, Vol. C-20, pp. 68-86, January 1971.
11. Breeding, K.J. and Ksienski, A.A., "The Inverse Scattering and Target Identification Problem," Tech. Rept. 2768-4, ElectroScience Laboratory, Dept. of E.E., The Ohio State University, Columbus, Ohio, November 1970.
12. Dudani, S.A., "Movement Methods for the Identification of Three Dimensional Objects from Optical Image," Tech. Rept., Communications and Control Systems Lab., Dept. of E.E., The Ohio State University, Columbus, Ohio, August 1971.
13. Seshu, S. and Reed, M.B., Linear Graphs and Electrical Networks, Addison Wesley, Reading, Mass., 1961.
14. Kruskal, J.B., "On the Shortest Spanning Subtree of a Graph and the Traveling Salesman Problem," Proc. Amer. Math Soc., No. 7, pp. 48-50, 1956.
15. Prims, R.C., "Shortest Connection Networks and Some Generalizations," Bell Sys. Tech. J., pp. 1389-1401, November 1957.
16. Gass, S.I., Linear Programming, McGraw-Hill, New York, 1964.

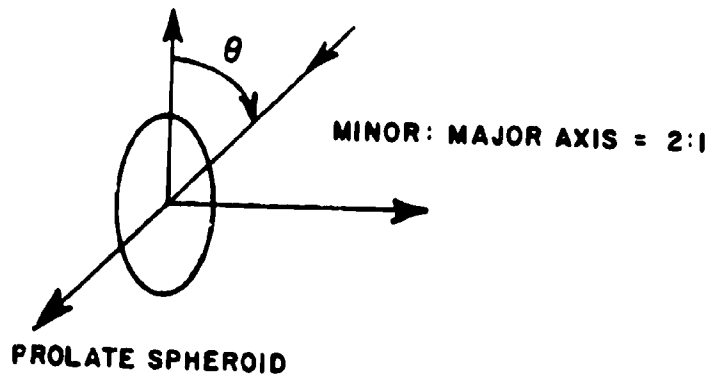
APPENDIX A



STEP CYLINDER



CYLINDER



PROLATE SPHEROID

Data File for Prolate Spheroid Horizontal Polarization

POINT	0	10	20	30	40	50	60
W 1	0.224940	0.225740	0.228070	0.231340	0.236030	0.241480	0.247120
W 2	0.666060	0.677670	0.711050	0.740770	0.806060	0.902650	1.07751
W 3	0.617900	0.658420	0.737980	0.869010	0.963980	1.10356	1.32460
W 4	0.826400G-01	0.644900G-01	0.736000G-01	0.214460	0.572760	0.827080	1.13065
W 5	0.643220	0.622500	0.552150	0.414680	0.231670	0.266790	0.592450
W 6	0.654160	0.683850	0.752540	0.807440	0.790450	0.675220	0.549330
W 7	0.898000G-02	0.544400G-01	0.233770	0.500370	0.782300	0.976320	1.03438
W 8	0.617510	0.590350	0.482310	0.249980	0.260080	0.719750	1.12260

POINT	70	80	90
W 1	0.254130	0.260540	0.263840
W 2	1.32389	1.56972	1.67894
W 3	1.65127	2.00871	2.17865
W 4	1.50888	1.90528	2.09285
W 5	0.992690	1.37982	1.55892
W 6	0.604730	0.815310	0.922790
W 7	1.02311	1.03279	1.04960
W 8	1.38108	1.53306	1.59029

Data File Cylinder (Original) Horizontal Polarization

POINT	0°	10°	20°	30°	40°	50°	60°
W 1	0.190000	0.190000	0.190000	0.190000	0.190000	0.190000	0.190000
W 2	0.610000	0.650000	0.630000	0.530000	0.550000	0.650000	0.610000
W 3	0.430000	0.460000	0.470000	0.470000	0.630000	0.810000	0.930000
W 4	0.410000	0.370000	0.280000	0.150000	0.160000	0.540000	0.910000
W 5	1.430000	1.410000	1.340000	1.160000	0.800000	0.340000	0.380000
W 6	1.280000	1.310000	1.380000	1.430000	1.280000	0.960000	0.500000
W 7	0.110000	0.900000G-01	0.320000	0.690000	0.930000	0.940000	0.720000
W 8	1.650000	1.540000	1.180000	0.630000	0.290000	0.440000	0.540000

POINT	70°	80°	90°
W 1	0.190000	0.190000	0.190000
W 2	0.670000	0.860000	0.990000
W 3	1.080000	1.320000	1.500000
W 4	1.290000	1.720000	1.870000
W 5	1.000000	1.610000	1.890000
W 6	0.720000	1.320000	1.610000
W 7	0.680000	1.070000	1.330000
W 8	0.700000	0.990000	1.150000

Scattering Data for Step Cylinder Horizontal Polarization

POINT	0	1	2	3	4	5	6	7	180
W 1	0.220367	0.344437	0.638380	0.822320	0.641987	0.389520	0.291419		
W 2	0.454440	1.16135	2.97550	3.95291	2.78435	0.934127	0.461653		
W 3	0.136693	0.631167	1.92957	2.84566	1.58333	0.152562	0.191513		
W 4	0.753793	0.894453	0.627560	2.26499	0.266172	1.33447	0.750187		
W 5	0.753793	1.21184	0.472473	2.16400	0.984620	0.696087	1.06397		
W 6	0.228663	0.389520	0.326043	1.63021	0.605920	0.652807	0.861993		
W 7	0.364273	0.789860	0.797073	2.23253	0.775433	2.04498	0.813960		
W 8	1.52923	0.602313	1.00626	2.30827	0.508540	1.26955	1.53283		